12. Beller GA, Watson DD. Physiological basis of myocardial perfusion imaging with the technetium-99m agents. *Semin Nucl Med* 1991;21:173–181.
13. Wackers FJ-TH, Berman DS, Maddahi J, et al. Technetium-99m-hexakis-2-methoxy-isobutyl isonitrile: human biodistribution, dosimetry, safety and preliminary comparison to thallium-201 for myocardial perfusion imaging. *J Nucl Med* 1989;30:301–311.
14. Baillet GY, Mena IG, Kuperus JH, et al. Simultaneous technetium-99m-MIBI angiography and myocardial perfusion imaging. *J Nucl Med* 1989;30:38–44.
15. Hayward JL, Rubens RD, Carbone PP, et al. Assessment of response to therapy in advanced breast cancer. A project of the program on Clinical Oncology of the UICC. *Eur J Cancer* 1978;14:1291–1292.
16. Hortobagyi GN, Blumenschein GR, Spanos W, et al. Multimodality treatment of locoregionally advanced breast cancer. *Cancer* 1983;51:763–768.
17. Buzdar A, Montague E, Baker J, et al. Management of inflammatory carcinoma of the breast with combined modality approach: an update. *Cancer* 1981;47:2537–2542.
18. Davila E, Vogel C. Management of locally advanced breast cancer (stage III): a review. *Int Adv Surg Oncol* 1984;7:1537–1543.
19. Hortobagyi GN, Ames FC, Buzdar AU, et al. Management of stage III primary breast cancer with primary chemotherapy, surgery and radiation therapy. *Cancer* 1988;62:2507–2516.
20. Abdel-Dayem HM, Scott AM, Macapinlac HA, et al. Role of ^{201}Tl and ^{99m}Tc-sestamibi in tumor imaging. In: Freeman, LM, ed. *Nuclear medicine annals*. New York: Raven Press; 1994:181–234.
21. Khalkhali I, Mena I, Diggles L. Review of imaging techniques for the diagnosis of breast cancer: a new role of prone scintimammography using technetium-99m-sestamibi. *Eur J Nucl Med* 1994;21:357–362.
22. Piwinica-Worms D, Chiu ML, Budding M, et al. Functional imaging of the multidrug-resistant P-glycoprotein with an organotechnetium complex. *Cancer Res* 1993;53:977–984.
23. Kedar RP, Cosgrove DO, Smith IE, et al. Breast carcinoma: measurement of tumor response to primary medical therapy with color Doppler flow imaging. *Radiology* 1994;190:825–830.

Iodine-123-α-Methyl Tyrosine in Gliomas: Correlation with Cellular Density and Proliferative Activity

Torsten Kuwert, Stefan Probst-Cousin, Burkhard Woesler, Carlo Morgenroth, Hartmut Lerch, Peter Matheja, Stefan Palkovic, Michael Schäfers, Hansdetlef Wassmann, Filippo Gullotta and Otmar Schober

Departments of Nuclear Medicine, Neuropathology and Neurosurgery, Westfälische Wilhelms-Universität Münster, Münster, Germany

Amino acid transport rate in gliomas can be assessed using SPECT and the amino acid L-^{123}I-α-methyl tyrosine (IMT). This study attempted to correlate the uptake of IMT by gliomas with the proliferative activity and cellular density of these neoplasms. **Methods:** The study used 27 patients with gliomas, including 18 patients with high-grade tumors and nine patients with low-grade neoplasms. Amino acid transport rate was determined using IMT and the triple-headed SPECT camera. Proliferative activity was immunohistochemically assessed as the relative number of cells expressing the Ki-67 nuclear antigen; cellular density was evaluated using light microscopy. **Results:** Relative IMT uptake correlated significantly with the proliferative fraction of tumor cells ($r = 0.6$, $p < 0.001$). There was no significant correlation between IMT uptake and cellular density ($r = 0.25$, $p > 0.05$). **Conclusion:** The uptake of the SPECT radiopharmaceutical IMT is related to proliferative activity rather than to the cellular density of gliomas.

Key Words: radionuclide imaging; gliomas; SPECT; iodine-123-α-methyl tyrosine; cellular density

J Nucl Med 1997; 38:1551–1555

The measurement of the regional uptake of radioactively labeled amino acids by SPECT or PET is a unique method for studying amino acid metabolism of brain tumors in vivo (*1–3*). The most widely used radiopharmaceutical for this purpose is the PET tracer ^{11}C-methionine; recently, ^{123}I-α-methyl tyrosine (IMT), another radioactively labeled amino acid, has been introduced as a radiopharmaceutical that is suitable for the less expensive and more available SPECT technique (*4–6*).

The uptake of ^{11}C-methionine and also of IMT has been shown to reflect amino acid transport rate (*6–10*), thus making it accessible to noninvasive investigation. In the field of brain tumors, the significance of these observations remains to be clarified because the relationship between amino acid transport rate and the biological behavior of gliomas is still unclear. This refers, in particular, to its correlation with the proliferative activity of these neoplasms.

Received Aug. 26, 1996; revision accepted Feb. 26, 1997.

For correspondence or reprints contact: Torsten Kuwert, MD, Department of Nuclear Medicine, Westfälische Wilhelms-Universität Münster, Albert-Schweitzer-Strasse 33, 48129 Münster, Germany.

It was the aim of our study to correlate IMT uptake, measured by preoperative SPECT, with the proliferative activity of gliomas, which was determined by using the immunohistochemical detection of the Ki-67 antigen. In addition, we also analyzed the relationship between IMT uptake and cellular density.

MATERIALS AND METHODS

Patients

Twenty-seven patients with untreated gliomas were entered into the study over a period of 18 mo. Informed consent was obtained from every subject studied. The study protocol had been approved by the Ethical Committee of the Westfälische Wilhelms-Universität.

Clinical and demographic data are detailed in Table 1. The average age of the patients (17 men and 10 women) was 55.9 yr (range, 34–82 yr). CT and/or T1- and T2-weighted magnetic resonance imaging (MRI) with intravenous contrast medium were obtained in all patients 8.6 days before surgery, on average (range, 0–32 days). On these images, we measured the two largest perpendicular transaxial diameters of the contrast-enhancing lesion; when the tumor exhibited no contrast enhancement (patients 19, 21 and 26), we determined the two largest perpendicular transaxial diameters of the whole CT or MRI abnormality in question. The two distances measured were then averaged for further analysis. Individual tumor sizes are listed in Table 1; the mean diameter of the tumors was 3.94 ± 1.6 cm.

Open surgery (17 cases) or stereotactic biopsy (10 cases) was performed 5.3 days after SPECT, on average, with a range of 1–19 days. None of the patients had biopsy before the SPECT investigation.

Histopathological assessment according to the criteria of the revised World Health Organization classification (*11*) revealed 13 astrocytomas IV, five astrocytomas III, seven astrocytomas II, one oligo-astrocytoma II and one subependymoma II (Table 1).

Immunohistochemistry

Formalin-fixed, paraffin-embedded specimens of each tumor were available for investigation. The evaluator was not aware of the clinical and SPECT data. Histological diagnosis and tumor grading had been performed independently by another examiner.

Immunohistochemistry was performed on 4-μm-thick sections, which were processed with an antibody to a formalin-resistant

TABLE 1
Patient Data

Patient no.	Age (yr)	Sex	Diagnosis	Surgery	IMT*	Size of ROI (cm^2)	Tumor diameter (cm)	Cell density (cells/HPF)	Ki-67† (%)
1	52	M	Astrocytoma IV	OP	3.68	2.54	3.5	426	25.9
2	53	F	Astrocytoma IV	OP	2.10	5.45	4.1	657	24.6
3	59	F	Astrocytoma IV	OP	1.62	7.35	4.4	511	17.5
4	55	M	Astrocytoma IV	OP	2.78	5.51	3.7	486	28.4
5	73	M	Astrocytoma IV	Biopsy	2.99	7.60	5.9	516	31.8
6	70	M	Astrocytoma IV	Biopsy	2.76	4.75	5.2	368	30.0
7	47	M	Astrocytoma IV	OP	1.95	5.32	3.7	361	17.0
8	72	M	Astrocytoma IV	OP	2.75	4.56	6.1	344	23.6
9	82	F	Astrocytoma IV	OP	1.76	9.89	2.5	848	32.0
10	40	F	Astrocytoma IV	OP	2.48	2.66	4.7	615	26.2
11	61	M	Astrocytoma IV	OP	2.17	5.01	2.6	455	43.2
12	66	F	Astrocytoma IV	Biopsy	1.81	6.08	3.8	529	24.3
13	53	M	Astrocytoma IV	OP	2.19	7.22	4.2	330	23.9
14	68	F	Astrocytoma III–IV	Biopsy	2.60	5.32	5.6	506	26.4
15	60	M	Astrocytoma III	Biopsy	2.10	3.87	5.0	332	9.5
16	36	M	Astrocytoma III	OP	1.64	3.42	2.3	466	42.2
17	54	F	Astrocytoma III	OP	1.90	4.44	2.7	385	22.4
18	58	M	Astrocytoma III	OP	4.00	3.61	3.5	310	40.9
19	59	M	Astrocytoma II	Biopsy	1.75	4.44	3.4	269	5.0
20	54	M	Astrocytoma II	Biopsy	1.91	5.51	4.3	144	0.6
21	34	M	Astrocytoma II	OP	1.16	5.00	2.9	265	2.0
22	49	M	Astrocytoma II	OP	1.78	3.93	1.9	230	6.6
23	44	M	Astrocytoma II	Biopsy	1.38	3.17	4.3	135	4.0
24	74	M	Astrocytoma II	Biopsy	1.67	8.68	2.7	125	1.4
25	37	F	Oligo-astrocytoma II	OP	1.94	5.76	8.9	290	5.1
26	35	F	Subependymoma II	OP	1.06	3.04	3.4	167	0.8
27	58	F	Glioma I–II	Biopsy	1.80	5.64	1.2	181	1.2

*Ratio between IMT uptake in tumor over uptake in reference ROI.
†Fraction of proliferating cells.
M = male; F = female; OP = operation.

epitope on the Ki-67 nuclear antigen (MIB1, 1:100). Antigen unmasking required microwave pretreatment, as described elsewhere (*12*). The avidin-biotin-peroxidase complex method was used, and the color reaction was developed with diaminobenzidine-tetrahydrochloride. Counting was performed using a high-power (×40) objective with a grid screen. The proliferative fraction of tumor cells was estimated establishing the MIB1 staining index as the percentage of MIB1 positive nuclei, of at least 1000 counted tumor cells from the areas of highest MIB1 staining, because counting areas exhibiting the highest concentration of positive labeling nuclei reduces statistical error (*13*).

Cell density was determined in representative areas by the investigation of 10 fields at high-power magnification on Nissl-stained sections and is presented as cells/high-power fields of view (HPF).

SPECT Data Acquisition

Details of the performance of IMT-SPECT in our laboratory have been described and discussed previously (*14,15*) so that only a brief description need be given here.

The patients fasted for at least 4 hr before IMT injection. SPECT was performed using the triple-headed camera MULTISPECT 3, which was equipped with medium-energy collimators (*16*). Imaging was started 10 min after intravenous injection of 110–130 MBq of IMT, synthesized and purified as reported previously (*14*); 96 views (3 × 32; 3.75°/step), each registered over 60 sec, were recorded into a 128 × 128 matrix format that corresponded to a pixel dimension of 3.56 × 3.56 mm^2 on a 360° rotation. Transaxial tomograms were reconstructed, without prefiltering, by using filtered back-projection. Attenuation correction was first-order, and it applied the method of Chang (*17*). In-plane resolution of the reconstructed images was 14 mm FWHM, and the slice thickness was approximately 7 mm.

Without knowledge of the clinical and histopathological data, regions of interest (ROIs) were manually defined on the two transaxial tomograms with the highest uptake of the lesion under study. As described and discussed in more detail previously (*14,15*), the ROIs placed on the lesions encompassed all pixels within that lesion with uptake values of greater than 90% of the maximum uptake in that slice. The further analysis resided on the average counting rate in each ROI. Individual ROI sizes are listed in Table 1; mean ROI size was 5.2 ± 1.8 cm^2.

Values of reference were obtained on the inferior of the two tomograms selected. For this purpose, we determined the mean IMT uptake from the hemispherical half that was not affected by the tumor or, when the tumor had crossed the midline, by the anterior or posterior half of that brain slice. Relative IMT uptake in the lesions was then determined by calculating ratios between the mean uptake in the two-lesion ROIs and that in the reference ROI.

Because of the semiautomated nature of this approach, the intra- and interobserver reproducibility of this method of regional analysis has been shown to be very high with correlation coefficients higher than 0.98, when relative uptake values were determined by two different observers or by the same observer, on two different days were compared (*14*). There was no significant correlation of IMT uptake with either ROI size ($r = -0.17$, $p > 0.05$) or tumor diameter ($r = 0.261$, $p > 0.05$).

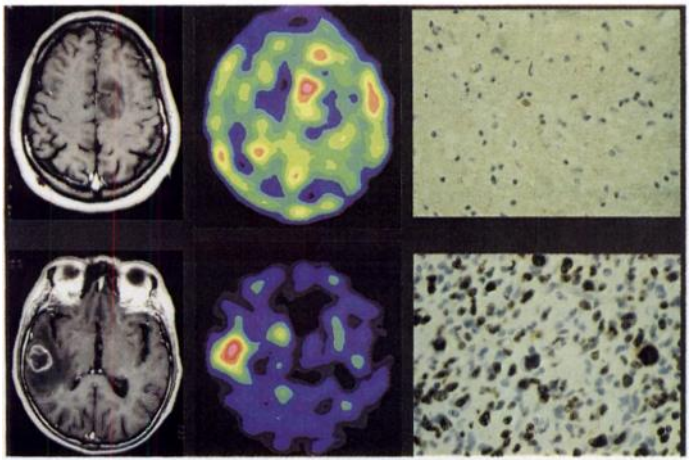

FIGURE 1. MRI, IMT-SPECT and Ki-67 stains in a patient with an astrocytoma II (top) and in a patient with an astrocytoma IV (bottom). Top left, transaxial, T1-weighted MRI (0.5 T) shows a hypointense nonenhancing lesion in the left frontodorsal lobe. Top middle, transaxial IMT-SPECT demonstrates low uptake in this astrocytoma II. The image is calibrated to its own maximum; red indicates the highest values. Top right, immunohistochemical staining of the astrocytoma II with Ki-67 antibody reveals a low proportion of proliferating (brown) cells (magnification, ×40). Bottom left, transaxial, T1-weighted MRI (1.5 T) shows an enhancing lesion in the right temporal lobe. Bottom middle, transaxial IMT-SPECT demonstrates high uptake in this astrocytoma IV. Bottom right, immunohistochemical staining of the astrocytoma IV with Ki-67 antibody reveals a high proportion of proliferating cells (magnification, ×40).

Data Analysis

All values are given as mean ± s.d. The distribution of all variables analyzed was compatible with normalcy as verified using Kolmogorov–Smirnoff one-sample tests. Means were compared using the Mann–Whitney U-test because there were major differences between subgroups with regard to s.d. Analyses of correlation were performed using Pearson's correlation coefficients and linear regression (*18*). This strategy was further supported by the finding that the use of nonparametric Kendall's tau resulted in no major change of the levels of significance compared to those demonstrated by parametric analysis.

RESULTS

Two representative examples of the patients who were studied are given in Figure 1. The individual IMT uptake values of the patients are listed in Table 1, together with the histopathological data.

Cell density, proliferative activity and IMT uptake were significantly lower in low-grade than in high-grade gliomas (Table 2). Proliferative activity and cell density were significantly correlated ($r = 0.69$, $p > 0.0001$; Fig. 2A). The correlation between IMT uptake and cell density was not significant ($r = 0.25$, $p > 0.05$; Fig. 2B). Relative IMT uptake correlated significantly with the fraction of proliferating tumor cells ($r = 0.60$, $p < 0.001$; Fig. 2C).

TABLE 2
Relationships of Histopathological Malignancy Grade with Cell Density, Proliferative Activity and IMT Uptake

	Low grade (n = 9)	High grade (n = 18)	Significance level*
Cell density (cells/HPF)	200.1 ± 64	469.1 ± 137	$p < 0.0001$
Proliferative activity (%)	3 ± 2.2	27.2 ± 8.74	$p < 0.0001$
IMT uptake	1.61 ± 0.33	2.4 ± 0.67	$p < 0.0017$

*Level of significance determined using the Mann–Whitney U-test.

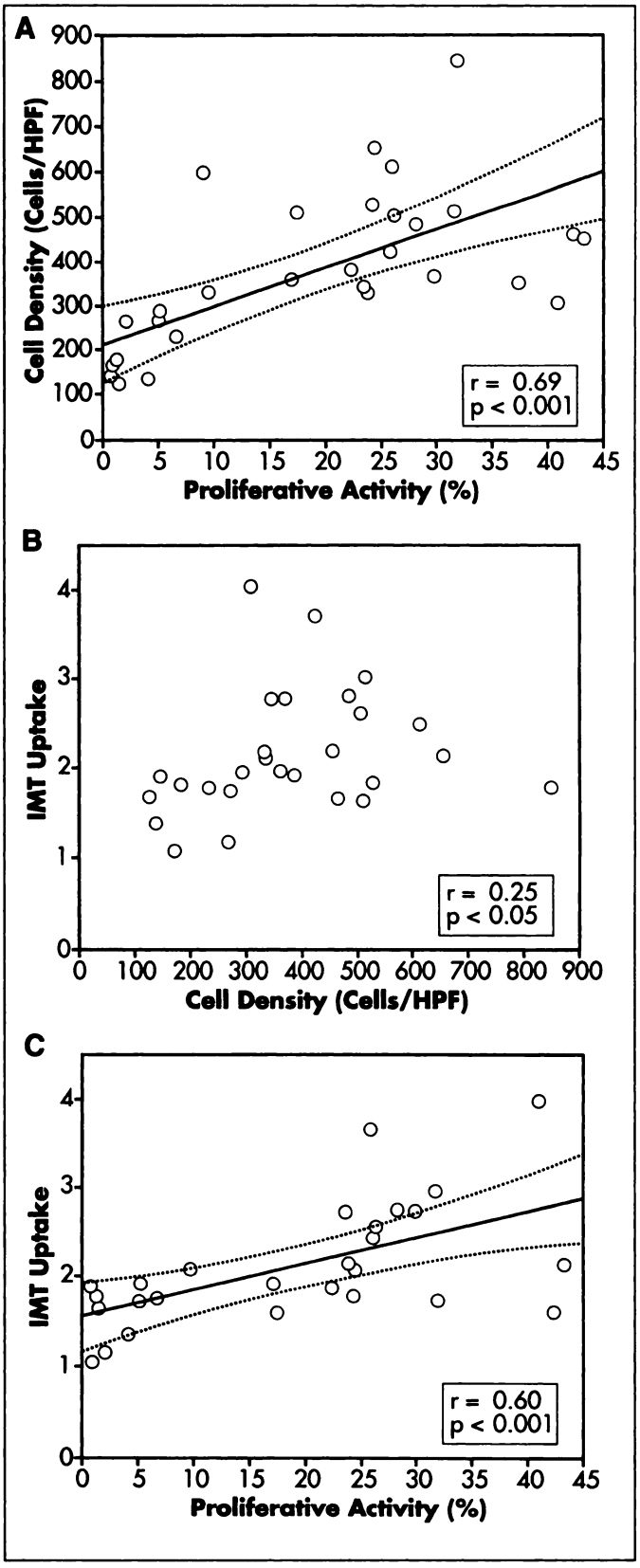

FIGURE 2. Plots of cell density compared to proliferative activity (A), relative IMT uptake compared to cell density (B) and relative IMT uptake compared to proliferative activity (C) in 27 gliomas. Dotted lines indicate 95% confidence limits for the mean.

DISCUSSION

The principal finding of this study is that the uptake of the SPECT radiopharmaceutical IMT correlates significantly with proliferative activity, but not with cell density of gliomas.

Several previous publications deal with the accumulation of radioactively labeled amino acids by gliomas. In particular, it has been shown that the uptake of amino acids by these tumors correlates with their histopathologically determined malignancy grade (*14,15,19–21*).

This observation is not completely understood. Regional values of radioactivity concentration measured by SPECT integrate over all cells contained in a particular volume of tissue, as it is defined by a ROI; therefore, the higher cellular density of high-grade gliomas compared to low-grade tumors (*22*) may explain the dependency of amino acid uptake on malignancy grade. There are indeed some reports in the literature favoring this hypothesis: Herholz et al. (*23*), for example, have shown that, in low-grade astrocytomas, the uptake of the PET tracer ^{18}F-fluorodeoxyglucose (FDG) correlates significantly with cellular density and not with histopathological signs of dedifferentiation; similarly, meningiomas with low cellular density may have lower FDG uptake than those with greater cellularity (*24*).

Our data do not support the contention that the higher amino acid uptake in high-grade gliomas than in low-grade gliomas is due to a higher cellularity of the former; this leads to the assumption that the cells of high-grade gliomas are more active with regard to amino acid transport than those of low-grade tumors.

This is also supported by in vitro studies demonstrating that amino acid uptake and, particularly, amino acid transport is increased in malignantly transformed cells compared to their untransformed parent cells (*25,26*). Probably, this is caused by the enhanced need of the more rapidly proliferating malignant cells for metabolic substrates; this hypothesis also provides an explanation for the observed significant correlation between proliferative activity and IMT uptake in our patients.

In brain tumors, the relationship between amino acid uptake and proliferative activity has not been previously studied. Our data are, however, in agreement with those reported for the uptake of the PET amino acid ^{11}C-methionine in peripheral tumors, e.g., in non-Hodgkin's lymphomas, non-small-cell lung carcinomas and breast cancers (*27–29*).

The values of cell density and proliferative activity reported herein correspond to those published by other authors (*30*), so our group of patients may be considered representative of larger groups of patients with gliomas. This is also illustrated by the significant relationship between histological grade, on one hand, and proliferative activity and cell density, on the other, in our patients, which is in agreement with previous publications (*30*).

Although the correlation between IMT uptake and proliferative activity was significant, the immunohistochemical parameter accounted only for approximately 36% of the variance of the SPECT data. In this context, limitations of the study design merit consideration; these concern the radiopharmaceutical used as well as physical constraints on imaging precision.

IMT uptake in gliomas is reduced by more than 50% when the serum level of the naturally occurring amino acids is raised (*6*); this and the observation that IMT is not incorporated into proteins (*5,7*) proves that at least 50% of this variable is due to specific transport phenomena. Unspecific binding cannot be excluded, as it contributes to the SPECT signal, possibly obscuring a closer correlation between amino acid uptake and biologic characteristics of the tumor than that observed in our study. Furthermore, IMT uptake values determined by SPECT are subject to partial volume errors, which leads to an underestimation of the real value when the size of the structure studied is smaller than twice the spatial resolution of the images analyzed (*14,31*). This is particularly important when tissue characteristics derived from the analysis of microscopic specimens are compared to the SPECT data, which integrate values from cells over several square centimeters of tissue. This difficulty could be circumvented using microautoradiographic techniques (*32*), which are difficult to apply in the human and were not available at our institution.

Whereas proliferative activity correlated significantly with IMT uptake, IMT uptake and cell density were poorly and, in this small group of subjects, not significantly correlated. In part, this may be due to technical difficulties in measuring the latter variable, which were caused by the well-known heterogeneity of gliomas with regard to cell size and type. With immunohistochemistry, the areas of greatest density of proliferating cells are immunohistochemically highlighted and may thus be defined with greater reproducibility (*30*) than the areas of greatest cell density on Nissl stains. Therefore, the histological heterogeneity of gliomas has lesser impact on the immunohistochemical determination of proliferative activity than on that of cell density. On the other hand, problems in accurately determining cell density would also obviate the demonstration of a significant relationship between cell density and proliferation rate. However, these variables were highly correlated in our group of patients; this suggests that technical difficulties in determining cell density exerted only a minor influence on our data.

A further SPECT radiopharmaceutical for studying brain tumors is ^{201}Tl. A significant correlation between uptake in gliomas and their proliferative activity has also been reported for this tracer; Oriuchi et al. (*33*), for example, demonstrated a significant correlation coefficient of 0.67 between relative ^{201}Tl uptake in 28 patients with supratentorial gliomas and proliferative activity determined using bromodeoxyuridine; Ishibashi et al. (*34*) recently published analogous data. However, it should be noted that the biochemical mechanisms governing ^{201}Tl uptake in gliomas have as yet not been elucidated; this renders the interpretation of ^{201}Tl uptake data more difficult than that for IMT. Besides the action of the $(Na^+\text{-}K^+)$-ATPase pump, unspecific factors such as damage to the blood–brain barrier and changes in blood flow or cellular density may also play a role in the accumulation of ^{201}Tl in tumor tissue (*35,36*). It would, therefore, be particularly interesting to compare ^{201}Tl uptake with cell density, which, as was also the case in our tumors, is correlated with proliferative activity and could thus also be responsible for the correlation between ^{201}Tl uptake and tumor proliferation.

CONCLUSION

The uptake of the SPECT radiopharmaceutical IMT correlates with proliferative activity rather than with cellular density of gliomas.

ACKNOWLEDGMENTS

We thank Maria Leisse and Heidi Gerdes-Funnekötter from the Institute of Neuropathology, University of Münster, for skillful technical assistance and for photographic services; Anne Exler, Christine Papenberg, Silke Steinhoff and Bernd Vollet from the Department of Nuclear Medicine, University of Münster, for their help with the SPECT camera; Dr. Wolfgang Brandau for synthesis of IMT; and the late Professor Peter E. Peters and Dr. Gerhard Schuierer from the Institute of Clinical Radiology, University of Münster, for their ongoing support.

REFERENCES

1. Herholz K. Tracers for clinical evaluation of gliomas: a neurologist's view. In: Mazoyer BM, Heiss WD, Comar D, et al., eds. *PET studies on amino acid metabolism and protein synthesis*. Dordrecht, The Netherlands: Kluwer Academic Publishers; 1993:203–214.
2. Conti PS. Introduction to imaging brain tumor metabolism with positron emission tomography. *Cancer Invest* 1995;13:244–259.

3. Leeds NE, Jackson EF. Current imaging techniques for the evaluation of brain neoplasms. *Curr Opin Oncol* 1994;6:254–261.
4. Biersack HJ, Coenen HH, Stöcklin G, et al. Imaging of brain tumors with L-3-[^{123}I]iodo-α-methyl tyrosine and SPECT. *J Nucl Med* 1989;30:110–112.
5. Langen KJ, Coenen HH, Roosen N, et al. SPECT studies of brain tumors with L-3-[^{123}I]iodo-α-methyl tyrosine: comparison with PET, ^{124}IMT and first clinical results. *J Nucl Med* 1990;31:281–286.
6. Langen KJ, Roosen N, Coenen HH, et al. Brain and brain tumor uptake of L-3-[^{123}I]iodo-α-methyl tyrosine: competition with natural L-amino acids. *J Nucl Med* 1991;32:1225–1228.
7. Kawai K, Fujibayashi Y, Saji H, et al. A strategy for the study of cerebral amino acid transport using iodine-123-labeled amino acid radiopharmaceutical: 3-iodo-alpha-methyl-L-tyrosine. *J Nucl Med* 1991;32:819–824.
8. Schober O, Meyer GJ, Stolke D, Hundeshagen H. Brain tumor imaging using ^{11}C-labeled L-methionine and D-methionine. *J Nucl Med* 1985;26:98–99.
9. Bergström M, Lundquist H, Ericson K, et al. Comparison of the accumulation kinetics of L-(methyl-^{11}C)-methionine and D-(methyl-^{11}C)-methionine in brain tumors studied with positron emission tomography. *Acta Radiol* 1987;28:225–229.
10. Ishiwata K, Kubota K, Murakami M, et al. Re-evaluation of amino acid PET studies: can the protein synthesis rates in brain and tumor tissues be measured in vivo? *J Nucl Med* 1993;34:1936–1943.
11. Kleihues P, Burger PC, Scheithauer BW. The new WHO classification of brain tumors. *Brain Pathol* 1993;3:255–268.
12. Cattoretti G, Becker MHG, Key G, et al. Monoclonal antibodies against recombinant parts of the Ki-67 antigen (MIB 1 and MIB 3) detect proliferating cells in microwave-processed formalin-fixed paraffin sections. *J Pathol* 1992;168:357–363.
13. Morimura T, Kitz K, Budka H. In situ analysis of cell kinetics in brain tumors. *Acta Neuropathol* 1989;77:276–282.
14. Kuwert T, Morgenroth C, Woesler B, et al. Uptake of iodine-123-α-methyl tyrosine by primary brain tumors and non-neoplastic brain lesions. *Eur J Nucl Med* 1996;23:1345–1353.
15. Kuwert T, Morgenroth C, Woesler B, et al. Influence of size of regions of interest on the measurement of uptake of iodine-123-α-methyl tyrosine by brain tumors. *Nucl Med Commun* 1996;17:609–615.
16. Kuikka JT, Tenhunen-Eskelinen M, Jurvelin J, Kiliänen H. Physical performance of the Siemens Multi SPECT 3 gamma camera. *Nucl Med Commun* 1993;14:490–497.
17. Chang LT. A method of for attenuation correction in radionuclide computed tomography. *IEEE Trans Nucl Sci* 1978;2:2780–2789.
18. Bortz J. *Lehrbuch der Statistik*, 2nd Ed. Berlin: Springer; 1985.
19. Schober O, Meyer G-J, Duden C, et al. Uptake of amino acids in brain tumours using positron emission tomography as an indicator for assessing metabolic activity and malignancy. *Fortsch Röntgenstr* 1987;147:503–509.
20. Derlon JM, Bourdet C, Bustany P, et al. Carbon-11-L-methionine uptake in gliomas. *Neurosurgery* 1989;25:720–728.
21. Ogawa T, Shishido F, Kanno I, et al. Cerebral glioma: evaluation with methionine PET. *Radiology* 1993;186:45–53.
22. Burger PC. The grading of astrocytomas and oligodendrogliomas. In: Fields WS, ed. *Brain tumors: a review of histologic classification*. New York: Springer, 1989:171–180.
23. Herholz K, Pietrzyk U, Voges J, et al. Correlation of glucose consumption and tumor cell density in astrocytomas. A stereotactic PET study. *J Neurosurg* 1993;79:853–858.
24. Cremerius U, Striepecke E, Henn W, et al. ^{18}FDG-PET in intracranial meningiomas versus grading, proliferation index, cellular density and cytogenetical analysis. *Nuklearmedizin* 1994;33:144–149.
25. Isselbacher KJ. Increased uptake of amino acids and 2-deoxy-D-glucose by virus-transformed cells in culture. *Proc Natl Acad Sci USA* 1972;69:585–589.
26. Saier MH Jr, Daniels GA, Boerner P, Lin J. Neutral amino acid transport systems in animal cells: potential targets of oncogene action and regulators of cellular growth. *J Membr Biol* 1988;104:1–20.
27. Leskinen-Kallio S, Ruotsalainen U, Nagren K, Teräs M, Joensuu H. Uptake of carbon-11-methionine and fluorodeoxyglucose in non-Hodgkin's lymphoma: a PET study. *J Nucl Med* 1991;32:1211–1218.
28. Miyazawa H, Arai T, Iio M, Hara T. PET imaging of non-small-cell lung carcinoma with carbon-11-methionine: relationship between radioactivity uptake and flow-cytometric parameters. *J Nucl Med* 1993;34:1886–1891.
29. Leskinen-Kallio S, Nagren K, Lehikoinen P, Ruotsalainen U, Joensuu H. Uptake of ^{11}C-methionine in breast cancer studied by PET. An association with the size of S-phase fraction. *Br J Cancer* 1991;64:1121–1124.
30. Lantos PL, Vandenberg SR, Kleihues P. Astrocytic tumours. In: Graham DJ, Lantos PL, eds. *Greenfield's neuropathology*, 6th Ed. London: Arnold; 1997:600–627.
31. Kuwert T, Sures T, Herzog H, et al. On the influence of spatial resolution and of the size and the form of regions of interest on the measurement of regional cerebral metabolic rates by positron emission tomography. *J Neural Transm* 1992;37(suppl):53–66.
32. Kubota R, Kubota K, Yamada S, et al. Methionine uptake by tumor tissue: a microautoradiographic comparison with FDG. *J Nucl Med* 1995;36:484–492.
33. Oriuchi N, Tamura M, Shibazaki T, et al. Clinical evaluation of thallium-201 SPECT in supratentorial gliomas: relationship to histological grade, prognosis and proliferative activities. *J Nucl Med* 1993;34:2085–2089.
34. Ishibashi M, Taguchi A, Sugita Y, et al. Thallium-201 in brain tumors: relationship between tumor cell activity in astrocytic tumor and proliferation cell nuclear antigen. *J Nucl Med* 1995;36:2201–2206.
35. Takekawa H, Itoh K, Abe S, et al. Thallium-201 uptake, histopathological differentiation and Na-K ATPase in lung adenocarcinoma. *J Nucl Med* 1996;37:955–958.
36. Tonami N. Thallium-201 SPECT in the evaluation of gliomas. *J Nucl Med* 1993;34:2089–2090.